Finite volume phases of large-*N* gauge theories with massive adjoint fermions

JHEP11(2009)008

(http://iopscience.iop.org/1126-6708/2009/11/008)

Published by IOP Publishing for SISSA

Received: *September 22, 2009*
Accepted: *October 13, 2009*
Published: *November 4, 2009*

Finite volume phases of large-N gauge theories with massive adjoint fermions

Timothy J. Hollowood and Joyce C. Myers

Swansea University, Physics Department,
Swansea SA2 8PP, U.K.

E-mail: t.hollowood@swansea.ac.uk, j.c.myers@swan.ac.uk

Abstract: The phase structure of QCD-like gauge theories with fermions in various representations is an interesting but generally analytically intractable problem. One way to ensure weak coupling is to define the theory in a small finite volume, in this case $S^3 \times S^1$. Genuine phase transitions can then occur in the large N theory. Here, we use this technique to investigate SU(N) gauge theory with a number N_f of massive adjoint-valued Majorana fermions having non-thermal boundary conditions around S^1. For $N_f = 1$ we find a line of transitions that separate the weak-coupling analogues of the confined and de-confined phases for which the density of eigenvalues of the Wilson line transform from the uniform distribution to a gapped distribution. However, the situation for $N_f > 1$ is much richer and a series of weak-coupling analogues of partially-confined phases appear which leave unbroken a $\mathbb{Z}_p$ subgroup of the centre symmetry. In these $\mathbb{Z}_p$ phases the eigenvalue density has p gaps and they are separated from the confining phase and from one-another by first order phase transitions. We show that for small enough mR (the mass of the fermions times the radius of the S^3) only the confined phase exists. The large N phase diagram is consistent with the finite N result and with other approaches based on $\mathbb{R}^3 \times S^1$ calculations and lattice simulations.

Keywords: Spontaneous Symmetry Breaking, Confinement, 1/N Expansion

ArXiv ePrint: 0907.3665

doi:10.1088/1126-6708/2009/11/008

JHEP11(2009)008

Contents

JHEP11(2009)008

1 Introduction

The study of gauge theories in finite volume, and specifically $S^3 \times S^1$, has been an interesting and fruitful one. A weak coupling regime is ensured by taking the size of the compact space to be small compared with the strong coupling scale, $\min[R_{S^1}, R_{S^3}] \ll \Lambda_{\rm QCD}^{-1}$. The theory is then non-trivial even at the one-loop level because the projection onto gauge invariant states introduces effective interactions between the gluons [1–4]. The large N limit is taken in order to ensure that a thermodynamic limit exists and genuine phase transitions occur. One motivation is to study thermal properties of gauge theories, in which case the S^1 is interpreted as the "thermal circle" and fermions have anti-periodic boundary conditions. A one-loop calculation is then sufficient to uncover the weak-coupling manifestation of the confinement/de-confinement transition in that on one side of the transition the expectation value of the Polyakov loop vanishes — the confining phase — while on the other side — the de-confined phase — it gains a VEV. The transition is Hagedorn-like in that the density of states grows exponentially in the low temperature phase. In order to ascertain the order of the transition higher loop effects are crucial [2]. In pure gauge theory it is known to be a first order transition that occurs at a lower temperature than the Hagedorn transition in the non-interacting theory. The same kind of transition occurs when adjoint matter fields are added, and in particular for the $\mathcal{N} = 4$ gauge theory. One of the deep insights to emerge from the AdS/CFT correspondence is that this transition can also be seen in the strong coupling gravity dual as a Hawking-Page transition from thermal AdS space to an

AdS black hole [5]. In the present paper, since we are interested in theories with periodic boundary conditions for fermions around the S^1 the phase transitions are quantum rather than thermal and the connection with the AdS/CFT correspondence is not so obvious even though one could imagine obtaining our theories from an $\mathcal{N} = 4$ theory with SUSY breaking mass deformations.

The phase diagram of SU(N) gauge theories in finite volume can be studied in other ways. At strong coupling lattice simulations are the dominant technique for obtaining the phase diagram. The phase diagrams using the strong and weak coupling techniques have so far not been easy to compare, since the relationship between lattice bare parameters and continuum renormalized parameters is not clear. However, in some cases a qualitative comparison is possible. In this paper we explore this possibility in adjoint QCD, that is, SU(N) gauge theory with fermions in the adjoint representation. The phase diagram of this theory is quite rich when considering $N_f > 1$ Majorana flavours with fermions of finite mass to which periodic boundary conditions have been applied in the temporal direction [6–12]. The intuition behind this is that the gauge field and fermion terms in the effective potential have opposite signs and compete to dominate the Polykov loop, with the fermions having a disordering effect. For a sufficient number of light fermions, the disordering effect dominantes and a confining phase results with vanishing Polakov loop, however as the masses are increased the disordering effect becomes weaker and a phase transition can occur where the centre symmetry is (partially) broken.

The issues that we investigate in this paper are relevant to some active areas of research. The application of periodic boundary conditions to adjoint representation fermions causes the confined phase to be accessible at weak coupling [6, 8, 13].[1] This is interesting for several reasons. For one, it is possible that observables may not differ significantly in the pure Yang-Mills theory confined phase and the perturbative confined phase of adjoint QCD. The latter feature might naïvely be inferred from the results of lattice calculations of the string tensions in the confining phase of the pure Yang-Mills theory which show little temperature dependence. However, it is also known that the string tensions have a significant temperature dependence above T_c in the de-confined phase [14]. This suggests an important question: Is the temperature dependence a result of the change in confinement scale when moving above T_c such that it would also occur in a high temperature confined phase, or is it something intrinsic to the de-confined phase? In the case where the high temperature confined phase is induced by periodic boundary conditions the question turns into one of dependence of observables on the length L of S^1 in the weak-coupling confined phase. In this case the question of temperature dependence becomes one of volume dependence.

The idea of volume dependence — or rather independence — is particularly interesting in the context of large N confining theories. In 1982 Eguchi and Kawai proposed volume independence in large N Yang-Mills theory in [15] where they employed large N factoriza-

[1] It should be noted that even though the confined phase is perturbatively accessible in adjoint QCD when $\min[R_{S^1}, R_{S^3}] \ll \Lambda^{-1}$, it was found in [32] that semiclassical analyses on $\mathbb{R}^3 \times S^1$, specifically including the contribution of magnetically charged objects in the confined phase, are only valid when $R_{S^1} N\Lambda \ll 1$. For certain observables which exhibit volume independence in the confined phase this should also be true on $S^3 \times S^1$. We thank Mithat Unsal for pointing out this important result.

JHEP11(2009)008

tion to show that pure Yang-Mills theory formulated on a lattice at some arbitrary volume, can be mapped onto the theory formulated on a single site. Around that time it was also shown that volume independence can only hold if certain symmetries are not broken, in particular it can only hold in the confining phase of large N gauge theories [16–19]. Several ideas were proposed to maintain the $\mathbb{Z}_N^d$ symmetry which is required on a space with d independently compactified dimensions (i.e. where certain dimensions $\mathbb{R}$ are compactified to S^1). Two of the most promising proposals were the quenched [17], and twisted [21] Eguchi-Kawai models. In the quenched EK model the eigenvalues of the Polyakov loop quenched, that is their eigenvalues are set by hand, such that $\mathbb{Z}_N^d$ symmetry required is explicit. However, results from lattice simulations of SU(N) gauge theory in [20] show that large N reduction using the quenched EK model breaks down. In the twisted EK model the boundary conditions are twisted by multiplying each plaquette in the lattice action by an element of the center such that the action becomes invariant under the required $\mathbb{Z}_N^d$ symmetry. The twisted EK model was shown to break down in [22, 23]. More recently, the idea of large N volume independence was picked up again and generalized in [13] where the authors proposed that since QCD(Adj) has a confined phase which is perturbatively accessible, a generalized Eguchi-Kawai large N reduction could relate the weak-coupling, small volume confined phase, to the strong coupling, large volume confined phase. Since this proposal there have been several tests. In [9] the authors performed a weak-coupling calculation of the effective potential for a three-dimensional adjoint matter theory which is related by generalized orbifold projection to QCD(Adj) in four dimensions with one dimension compact. In [11] it was shown that this calculation is renormalization scheme dependent and that for Eguchi-Kawai reduction to hold it requires double trace counter-terms with coefficients defined so that the $\mathbb{Z}_N$ symmetry is preserved in the limit of zero adjoint fermion mass. In a lattice simulation [10] for $N = 3$ the authors calculated the phase diagram of QCD(Adj) on a $16^3 \times L_c$ lattice and showed that there is a confined phase at both strong and weak coupling but that they are separated by phase transitions into other phases depending on the value of the adjoint fermion mass. From their results the presence, or lack thereof, of phase transitions in the chiral limit is unclear. But, their result places boundaries on the validity of large N reduction either way since it can only hold when the theories to be mapped are in confining phases. Most recently in [12] the Eguchi-Kawai reduced (single-site) model with dynamical adjoint fermions was studied on the lattice and it was shown that the $\mathbb{Z}_N$ symmetry is unbroken for light enough fermion mass. Some applications of Eguchi-Kawai reduction can be found in [24, 25] where the authors use large N reduction of SYM ($\mathcal{N} = 1$ in [24] and $\mathcal{N} = 4$ in [25]) on $S^3 \times \mathbb{R}$ to reduce the theory to a single dimension for the purpose of studying supersymmetric matrix quantum mechanics.

Our calculations in this paper place boundaries on validity of large-N reduction at weak coupling and finite fermion mass by mapping the regions of $Z(N)$ symmetry breaking in the phase diagram of large N adjoint QCD. The phase diagram is calculated as a function of the length L of S^1, the radius R of S^3, and the adjoint fermion mass m. In particular, for small L/R the mass of the fermions, times the radius R, must be below a critical value to keep the theory in a $Z(N)$ symmetric phase. It is clearly an important question to

JHEP11(2009)008

understand the phases of QCD with adjoint fermions as a function of the volume and mass and it is to this question that we now turn.

In section 2 we compute the effective action for the theory on $S^3 \times S^1$ as a function of the Polyakov loop to one-loop order paying particular attention to the inclusion of a mass for the fermions. Section 3 investigates the phase diagram of the large N theory as a function of the radii of $S^3 \times S^1$ and the mass of the fermions and for different numbers of adjoint fermion flavours. Here we show the existence of a rich phase structure for $N_f > 1$. In the final section, we consider the same theories with N finite where the phase transitions are no longer non-analytic but allow comparisons with with earlier work mentioned above for the theory on $\mathbb{R}^3 \times S^1$ and lattice simulations.

2 The effective action on $S^3 \times S^1$

In this section, we review the way that the effective action is calculated on $S^3 \times S^1$ to the level of the one-loop approximation. The only new ingredient over earlier work is the inclusion of a mass for the fermions. Our approach follows closely the philosophy set out in the beautiful paper [1], however, we shall use a more conventional form of gauge fixing, described in [26–28], that leads to the same result.

We shall start with SU(N) gauge theory with a number of Majorana fermions ψ_f transforming in representations R_f of the gauge group.[2] The action is

$$S = \frac{1}{g^2_{\rm YM}} \int d^4x \sqrt{g} \left\{ -\frac{1}{4} \mathrm{Tr}\, F_{\mu\nu} F^{\mu\nu} + \sum_{f=1}^{N_f} \left(i \bar{\psi}_f \not{D} \psi_f - m_f \bar{\psi}_f \psi_f \right) \right\} \tag{2.1}$$

and the covariant derivatives are appropriate to the representation R_f.

The problem before us is to compute a Wilsonian effective action for the gauge theory on $S^3 \times S^1$ to the one loop order. We denote the length of S^1 by L and the radius of S^3 by R. The only zero modes in the set-up belong to A_0, the gauge field component around S^1:

$$\alpha = \frac{1}{\mathrm{Vol}\, S^3 \times S^1} \int_{S^3 \times S^1} A_0 \ . \tag{2.2}$$

We can use a global gauge transformation to diagonalize α:

$$\alpha = L^{-1} \mathrm{diag}(\theta_i) \ . \tag{2.3}$$

The θ_i are angular variables since there are large gauge transformations (but periodic around S^1) that take $\theta_i \to \theta_i + 2\pi$. Physically, the gauge invariant quantities are built out of the Wilson loop $P = e^{iL\alpha}$ (the Polyakov loop in the case of thermal boundary conditions) evaluated in the fundamental representation:[3]

$$\mathrm{Tr}\, P^n = \sum_{j=1}^{N} e^{in\theta_j} \ , \tag{2.4}$$

[2] In general in order to have a mass term the representations R_f must be real or include complex conjugate pairs. In the case here we are considering the adjoint representation which is real.

[3] Unless otherwise specified, traces are taken in the fundamental representation.

JHEP11(2009)008

On top of this there are additional large gauge transformations that are only periodic on S^1 up to a subgroup of the centre $\mathbb{Z}_N$ depending on the matter content of the theory. For adjoint matter, this subgroup is the whole of $\mathbb{Z}_N$ and so non-periodic large gauge transformations take $\theta_i \to \theta_i + 2\pi/N$ and so transform $\mathrm{Tr}P$ by an N-th root of unity. Hence, strictly speaking, the gauge invariant observables are, for example, $|\mathrm{Tr}P|$.

The radiative corrections at the one loop level are obtained by taking the constant mode (2.3) as a background VEV and integrating out all the massive modes of the fields. To this end, we shift $A_0 \to A_0 + \alpha$ and then the one-loop contribution involves the logarithm of the resulting functional determinants which depend on α in a non-trivial way. As usual we have to fix the gauge in some way and we prefer to use a different and more conventional approach than that of [1]. To this end we impose Feynman gauge by adding the standard gauge fixing term

$$S_{\mathrm{gf}} = \frac{1}{g_{\mathrm{YM}}^2}\frac{1}{2}\int d^4x\sqrt{g}\,\mathrm{Tr}\Big(\nabla_i A^i + \tilde{D}_0 A_0\Big)^2, \tag{2.5}$$

and appropriate ghosts. To the one loop level, we expand the action to quadratic order in fluctuations. The gauge field part of the action, including the ghosts, is

$$\begin{aligned} S_{\mathrm{gauge}} = \frac{1}{g_{\mathrm{YM}}^2}\int d^4x\sqrt{g}\,\mathrm{Tr}\,\Big[&\frac{1}{2}A_0(-\tilde{D}_0^2 - \Delta^{(s)})A_0 \\ &+ \frac{1}{2}A_i(-\tilde{D}_0^2 - \Delta^{(v)})A^i + +\bar{c}(-\tilde{D}_0^2 - \Delta^{(s)})c\Big]\,. \end{aligned} \tag{2.6}$$

Here, $\Delta^{(s)}$ and $\Delta^{(v)}$ are the Laplacians on S^3 for scalar and gauge fields, respectively. The scalar Laplacian is simply $\Delta^{(s)} = g^{-1/2}\partial_\mu(g^{1/2}\partial^\mu)$ whilst the vector Laplacian is

$$\Delta^{(v)}A^i = \nabla_j\nabla^j A^i - R^i{}_j A^j\,, \tag{2.7}$$

where R_{ij} is the Ricci tensor of S^3. In the above, $\tilde{D}_0 = \partial_0 + i\alpha$ and so includes the coupling to the VEV.

Each fluctuating field is expanded in terms of appropriate harmonics on $S^3 \times S^1$ and a typical contribution to the effective action is of the form

$$\pm\,\mathrm{Tr}_R\log(-\tilde{D}_0^2 - \Delta)\,, \tag{2.8}$$

the ± 1 being for c-number and Grassmann fluctuations, respectively and Δ is the Laplacian on S^3 appropriate to the tensorial nature of the field on S^3; either $\Delta^{(s)}$, $\Delta^{(v)}$ or $\Delta^{(f)}$. The background VEV α acts as a generator of the Lie algebra of SU(N) in the representation R of the gauge group appropriate to the field and the trace includes a trace over that representation of the gauge group. The eigenvalues of ∂_0 are simply $2\pi i n/L$, $n \in \mathbb{Z}$, while the eigenvectors of the Laplacian on S^3 are labelled by the angular momentum ℓ:

$$\Delta\psi_\ell = -\varepsilon_\ell^2\psi_\ell\,, \tag{2.9}$$

and we denote their degeneracy as d_ℓ. The ε_ℓ and d_ℓ depend on the field type. We review the spectra of the appropriate Laplacians on an arbitrary sphere in appendix A. For us, the relevant fields are scalars (more precisely minimally coupled scalars), vectors and spinors and below we list the relevant data:

JHEP11(2009)008

field	angular mom.	energy	degeneracy
B_i	$\ell > 0$	$(\ell+1)/R$	$2\ell(\ell+2)$
C_i	$\ell > 0$	$\sqrt{\ell(\ell+2)}/R$	$(\ell+1)^2$
$\bar{c}, c$	$\ell \geq 0$	$\sqrt{\ell(\ell+2)}/R$	$-2(\ell+1)^2$
A_0	$\ell \geq 0$	$\sqrt{\ell(\ell+2)}/R$	$(\ell+1)^2$
ψ_α	$\ell > 0$	$\sqrt{(\ell+\frac{1}{2})^2 + m^2R^2}/R$	$-2\ell(\ell+1)$

Table 1. The fields, their angular momenta, energy and degeneracy (with $\pm$ sign for c-number and Grassmann fluctuations) in the effective action. The fermion result is for a massive Majorana fermion on $S^3 \times S^1$.

(i) *Scalars.* For minimally coupled scalars $\varepsilon_\ell = R^{-1}\sqrt{\ell(\ell+2)}$ and the degeneracy $d_\ell = (\ell+1)^2$ with $\ell \geq 0$.

(ii) *Spinors.* For the irreducible 2-component real spinors,[4] we have $\varepsilon_\ell = R^{-1}(\ell+1/2)$ and $d_\ell = \ell(\ell+1)$ with $\ell > 0$.

(iii) *Vectors.* Here the situation is more complicated. A vector field V_i can be decomposed into the image and the kernel of the covariant derivative: $V_i = \nabla_i\chi + B_i$, with $\nabla^i B_i = 0$. The eigenvectors for the "transverse part", B_i, have $\varepsilon_\ell = R^{-1}(\ell+1)$ and $d_\ell = 2\ell(\ell+2)$ with $\ell > 0$. On the other hand, the "longitudinal part" $\nabla_i\chi$ has $\varepsilon_\ell = R^{-1}\sqrt{\ell(\ell+2)}$ with degeneracy $d_\ell = (\ell+1)^2$ but with $\ell > 0$ only.

It is a standard calculation using the identity $\prod_{n=1}^{\infty}(1+x^2/n^2) = \sinh(\pi x)/(\pi x)$ to show that (2.8) is equal, up to an infinite additive constant, to

$$\sum_{\ell=0}^{\infty} d_\ell \Big\{ L\varepsilon_\ell - 2\sum_{n=1}^{\infty} \frac{1}{n} e^{-nL\varepsilon_\ell} \mathrm{Tr}_{\mathrm{R}}\big(P^n\big) \Big\} \ . \tag{2.10}$$

The first term here involves the Casimir energy and since it is independent of α will play no rôle in our story and we will subsequently drop it.

Notice that the $\ell > 0$ contributions from A_0, C_i and the ghosts all cancel leaving only a net contribution from the $\ell = 0$ modes of the form[5]

$$\sum_{n=1}^{\infty} \frac{1}{n} \mathrm{Tr}_{\mathrm{adj}}\big(P^n\big) \ . \tag{2.12}$$

[4] A Majorana spinor on $S^3 \times S^1$ corresponds to 2 such spinors on S^3.

[5] This part is precisely the exponentiation of the Jacobian that converts the integrals over the θ_i into an integral over the unitary matrix $P = \mathrm{diag}(e^{i\theta_i})$:

$$\int \prod_{i=1}^{N} d\theta_i \, \exp\Big\{ \sum_{n=1}^{\infty} \frac{1}{n} \mathrm{Tr}_{\mathrm{adj}}\big(P^n\big) \Big\} \propto \int \prod_{i=1}^{N} d\theta_i \prod_{i<j} \sin^2\Big(\frac{\theta_i - \theta_j}{2}\Big) = \int dP \ . \tag{2.11}$$

However, we will leave the Jacobian in the exponent since it must be considered as part of the effective action for the eigenvalues.

JHEP11(2009)008

The remaining gauge modes are the vector modes B_i and the fermions. Using the sum (2.10) and including the Jacobian term in (2.12), the full effective action is then

$$S(\alpha) = \sum_{n=1}^{\infty} \frac{1}{n} \Big\{ \big(1 - z_v(nL/R)\big) \mathrm{Tr}_{\mathrm{adj}}\big(P^n\big) + \sum_{f=1}^{N_f} z_f(nL/R, m_f R) \mathrm{Tr}_{R_f}\big(P^n\big) \Big\} \,. \tag{2.13}$$

In the above, we have defined

$$z_v(L/R) = 2\sum_{\ell=1}^{\infty} \ell(\ell+2) e^{-L(\ell+1)/R} = \frac{6e^{-2L/R} - 2e^{-3L/R}}{(1-e^{-L/R})^3} \,, \tag{2.14}$$

and for the spinors

$$z_f(L/R, mR) = 2\sum_{\ell=1}^{\infty} \ell(\ell+1) e^{-L\sqrt{(\ell+1/2)^2 + m^2R^2}/R} \,. \tag{2.15}$$

We have assumed that the fermions have periodic boundary conditions around S^1. If one wanted to describe the case of finite temperature the fermions have anti-periodic boundary conditions and $z_f(nL/R, m_f R)$ must be multiplied by an additional factor of $(-1)^n$.

Notice for the vector modes, we are able to perform the sum over the angular momentum, but for the fermion modes this is not possible due to the non-zero mass. However, a useful expression for the fermionic contribution can be obtained by applying a version of the Abel-Plana formula which is proved in appendix B appropriated to a function with branch points on the imaginary axis:

$$\sum_{\ell=0}^{\infty} f(\ell + \frac{1}{2}) = \int_0^{\infty} dx\, f(x) - i \int_0^{\infty} dx\, \frac{f(ix+\varepsilon) - f(-ix-\varepsilon)}{e^{2\pi x}+1} \,. \tag{2.16}$$

In the above ε is positive, real, and infinitesimal. Applying this formula to the function

$$f(\ell) = 2\ell(\ell+1/2) e^{-L\sqrt{(\ell+1/2)^2 + m^2R^2}/R} \,, \tag{2.17}$$

gives the integral representation

$$\begin{aligned} & z_f(L/R, mR) \\ &= 2\int_0^{\infty} dx \left(x^2 - \frac{1}{4}\right) e^{-L\sqrt{x^2+m^2R^2}/R} + 4\int_{mR}^{\infty} dx \frac{x^2+\frac{1}{4}}{e^{2\pi x}+1} \sin\left(L\sqrt{x^2-m^2R^2}/R\right) \\ &= \frac{2m^2R^3}{L} K_2(Lm) - \frac{mR}{2} K_1(Lm) + 4\int_{mR}^{\infty} dx \frac{x^2+\frac{1}{4}}{e^{2\pi x}+1} \sin\left(L\sqrt{x^2-m^2R^2}/R\right) \,. \end{aligned} \tag{2.18}$$

Note that in our case the function $f(ix)$ is real for $x < mR$ and becomes imaginary for $x > mR$ and so the lower limit of the second integral has been taken to be mR.

There are two consistency checks we can make on the integral expression (2.18). Firstly, in the massless limit, $m \to 0$, we have

$$z_f(L/R, 0) = \frac{4e^{-3L/2R}}{(1-e^{-L/R})^3} \equiv \sum_{\ell=1}^{\infty} 2\ell(\ell+1) e^{-L(\ell+1/2)/R} \,. \tag{2.19}$$

Secondly in the limit $R \to \infty$ with fixed m and L, we have

$$z_f(L/R, mR) \longrightarrow \frac{2m^2R^3}{L} K_2(Lm)\,, \tag{2.20}$$

which is the expression that one obtains by working directly on $\mathbb{R}^3 \times S^1$ [8].

3 Phase structure of QCD(Adj)

In this section, we apply our result (2.13) to the particular case of a theory with N_f adjoint fermions with equal masses. In this case, we have

$$\mathrm{Tr}_{\mathrm{adj}}\big(P^n\big) = \sum_{ij=1}^{N} \cos(n(\theta_i - \theta_j)) \tag{3.1}$$

and so

$$S(\theta_i) = \sum_{n=1}^{\infty} \frac{1}{n}\Big(1 - z_v(nL/R) + N_f z_f(nL/R, m_f R)\Big) \sum_{ij=1}^{N} \cos(n(\theta_i - \theta_j))\ . \tag{3.2}$$

The phase structure is determined by minimizing this with respect to the $\{\theta_i\}$. Since N is large, it is more appropriate to describe the configuration in terms of a density $\rho(\theta)$ normalized so that

$$\int_0^{2\pi} d\theta\, \rho(\theta) = 1\ . \tag{3.3}$$

In this case, we can write the effective action as

$$S[\rho(\theta)] = N^2 \int d\theta \int d\theta'\, \rho(\theta)\rho(\theta') \sum_{n=1}^{\infty} \frac{f(nL/R, mR)}{n} \cos(n(\theta - \theta')) \tag{3.4}$$

In the above, we have defined the function

$$f(L/R, mR) = 1 - z_B(L/R) + N_f z_F(L/R, mR)\ . \tag{3.5}$$

It is useful to Fourier analyze the density:

$$\rho(\theta) = \frac{1}{2\pi} \sum_{n=-\infty}^{\infty} \rho_n e^{-in\theta}\,, \tag{3.6}$$

with $\rho_0 = 1$ and $\rho_n^* = \rho_{-n}$ for reality. The action then becomes

$$S[\rho(\theta)] = N^2 \sum_{n=1}^{\infty} \frac{f(nL/R, mR)}{n} |\rho_n|^2 \tag{3.7}$$

The phase structure hinges on properties of the function $f(L/R, mR)$ and specifically on its sign. For large L/R and any m, both $z_B, z_F \to 0$ and so $f(L/R, mR) \to 1$. The behaviour in the limit of small L/R depends on how m is scaled. If we keep mL fixed then

$$f(L/R, mR) \longrightarrow \frac{2m^2R^3}{L}\left(N_f K_2(mL) - \frac{2}{(mL)^2}\right)\ . \tag{3.8}$$

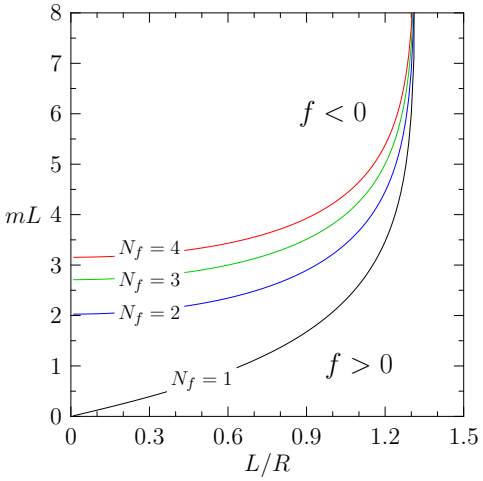

Figure 1. The lines where $f = 0$ indicating the regions where $f > 0$ and $f < 0$ in the $(L/R, mL)$ plane for $N_f = 1, \ldots, 4$.

In this limit, f is positive (negative) for $mL < a$ ($mL > a$), where a is the solution of

$$N_f a^2 K_2(a) = 2\,, \tag{3.9}$$

which is only possible if $N_f > 1$. For $N_f = 1$, f is negative for all mL (in the limit of small L/R). If we consider small L/R but keep mR fixed then

$$f(L/R, mR) \longrightarrow \frac{4R^3}{L^3}(N_f - 1) - \frac{m^2 R^3 N_f}{L} + \cdots\ . \tag{3.10}$$

Note that this is positive for $N_f > 1$.

It will be useful to chart the phase diagram initially in the $(L/R, mL)$ plane and in figure 1 we show the corresponding regions for which f is positive and negative, for $N_f = 1, 2, 3, 4$.

Having charted the region where f is positive and negative we can now build up a picture of the phase structure. It will be useful to define $f_n \equiv f(nL/R, mR)$ so that

$$S = N^2 \sum_{n=1}^{\infty} \frac{f_n}{n} |\rho_n|^2\ . \tag{3.11}$$

In the region where all the $f_n > 0$, $n = 1, 2, \ldots$, it is clear that the action will be minimized when all the Fourier modes vanish $\rho_n = 0$, except $\rho_0 = 1$, *i.e.* $\rho(\theta) = 1/2\pi$. This phase is the weak-coupling manifestation of the confining phase where the centre symmetry is unbroken and $\mathrm{Tr}P^n = 0$, $n > 0$. In view of this we will call it the "confining phase".

The confining phase covers the region of the phase diagram where all the $f_p > 0$. This is separated from the rest of the phase diagram by the union of arcs where a given f_p vanishes. The arc where $f_p = 0$ extends between 2 multi-critical points where $f_p = f_{p+1} = 0$ and $f_{p-1} = f_p = 0$, respectively. As one crosses the contour on which $f_p = 0$ a phase transition occurs where the density $\rho(\theta)$ develops p gaps, that is p intervals around the circle on which

JHEP11(2009)008

$\rho(\theta)$ vanishes. We call the resulting phase the $\mathbb{Z}_p$ phase since at strong coupling it would be identified with a partially confined phase where the SU(N) gauge group is broken to a subgroup SU(p) that confines and a $\mathbb{Z}_p$ subgroup of the centre symmetry remains unbroken. The signature of the $\mathbb{Z}_p$ phase is that the order parameters behave as

$$\begin{aligned} \mathrm{Tr}\, P^n &= 0\,, \qquad n/p \notin \mathbb{Z}\,, \\ \mathrm{Tr}\, P^n &\neq 0\,, \qquad n/p \in \mathbb{Z}\,. \end{aligned} \tag{3.12}$$

The detailed argument of why such a transition occurs follows as a generalization of the transition from the uniform to one gap phase described in [1] and we include it for completeness. The important point is that the configuration space $\{\rho_n\}$ has a non-trivial boundary which encloses the allowed region surrounding the origin because the density $\rho(\theta)$ cannot be negative. The boundary region consequently consists of distributions for which $\rho(\theta)$ vanishes at a subset of points (including finite intervals) around the circle. Furthermore, it is clear that allowed region in the configuration space is a convex region, since if $\rho_1(\theta)$ and $\rho_2(\theta)$ are allowed then so is $t\rho_1(\theta) + (1-t)\rho_2(\theta)$, $0 \leq t \leq 1$.

Let us consider the transition across the line where $f_p = 0$. On the confining phase side of the transition $f_p > 0$ and $\rho(\theta) = 1/2\pi$. At the transition point, the action becomes independent of the Fourier component ρ_p and so the one complex parameter family of densities

$$\rho(\theta) = \frac{1}{2\pi}\left(1 + \rho_p e^{-ip\theta} + \rho_p^* e^{ip\theta}\right) \tag{3.13}$$

for $0 \leq |\rho_p| \leq \frac{1}{2}$ all have the same (vanishing) action. As f_p becomes negative, then the points with $S = 0$ in the configuration space is a cone whose angle opens as f_p becomes more negative. The locus of configurations with $S < 0$ correspond to hyperbolae lying inside this cone. It follows that the configuration with minimal action lies on the boundary of the configuration space at a point where one of the hyperbola lies tangent to the boundary, i.e. on a distribution where $\rho(\theta)$ vanishes at a subset of points. This is illustrated in figure 2. We conclude that new configuration is continuously connected to the $|\rho_p| = \frac{1}{2}$ density in (3.13) and so must have precisely p gaps. By symmetry this phase will be invariant under a $\mathbb{Z}_p$ subgroup of the centre symmetry. A schematic view of the transition appears in figure 3. The transition is first order since the effective action is discontinuous across the transition. In the confining phase we have $S = 0$, whereas just above the transition to leading order it is sufficient to take the density to be (3.13) with $|\rho_p| = \frac{1}{2}$ and plug this into the action to get

$$S = \frac{N^2}{4p} f_p(L/R, mR)\,, \tag{3.14}$$

because the density itself only changes at a higher order. Since $f_p(L/R, mR)$ has non-vanishing first derivatives in δL and δm^2 the derivatives of S change discontinuously across the transition implying that it is first order.

As we remarked above the critical lines $f_p = 0$ and $f_{p+1} = 0$ cross at multi-critical points where $f_p = f_{p+1} = 0$, and at these points the confining, $\mathbb{Z}_p$ and $\mathbb{Z}_{p+1}$ phases are all

JHEP11(2009)008

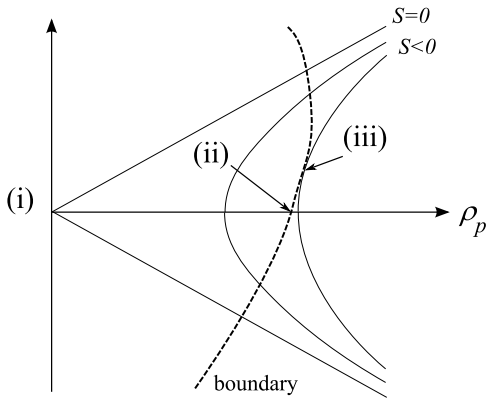

Figure 2. The structure of configuration space showing $|\rho_p|$ and one additional direction. The boundary is indicated by the dotted line and it is important that the allowed region is convex. For $f_p < 0$, the lines of vanishing action define a cone and the lines of constant negative action being hyperbolae therein. The density (i) is the uniform distribution characteristic of the confining phase; (ii) is the density with $|\rho_p| = \frac{1}{2}$ which lies at the boundary of configuration space; and (iii) is the density with minimal action as lying at the boundary of configuration space where the lines of constant S lie tangent to boundary.

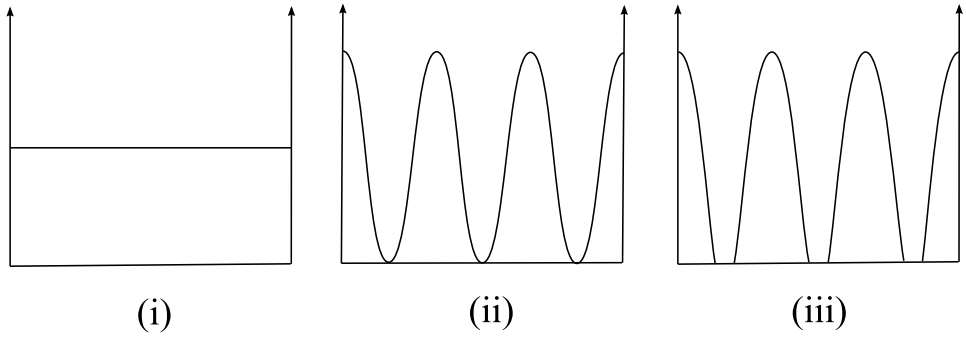

Figure 3. The behaviour of the density across the transition at $f_p = 0$: (i) the uniform density in the confining phase and (iii) the $\mathbb{Z}_p$ phase (for $p = 3$). At the transition point (ii) the mode ρ_p becomes massless and the density develops p zeros as shown in the middle.

continuously connected via the density

$$\rho(\theta) = \frac{1}{2\pi}\left(1 + \rho_p e^{-ip\theta} + \rho_p^* e^{ip\theta} + \rho_{p+1} e^{-i(p+1)\theta} + \rho_{p+1}^* e^{i(p+1)\theta}\right) . \tag{3.15}$$

By continuity, it must be that there are lines of first order phase transitions that separate the partially confined phases and which end on the critical points that lie somewhere between the continuation of the $f_p = 0$ and $f_{p+1} = 0$ lines.[6] The actual positions of these lines of transition will depend in detail on the gapped distributions. However, in the limit $R \to \infty$ with m and L fixed, we know from (3.8) that up to an overall factor

[6]The argument is as follows, in the vicinity of the critical point we have $S = N^2 f_p/4p$ and $N^2 f_{p+1}/4(p+1)$, respectively, in the $\mathbb{Z}_p$ and $\mathbb{Z}_{p+1}$ phases. A first order transition occurs when $f_p/p = f_{p+1}/(p+1)$ which must necessarily be in a region where $f_p < 0$ and $f_{p+1} < 0$, in other words somewhere between the continuations of the $f_p = 0$ and $f_{p+1} = 0$ lines.

JHEP11(2009)008

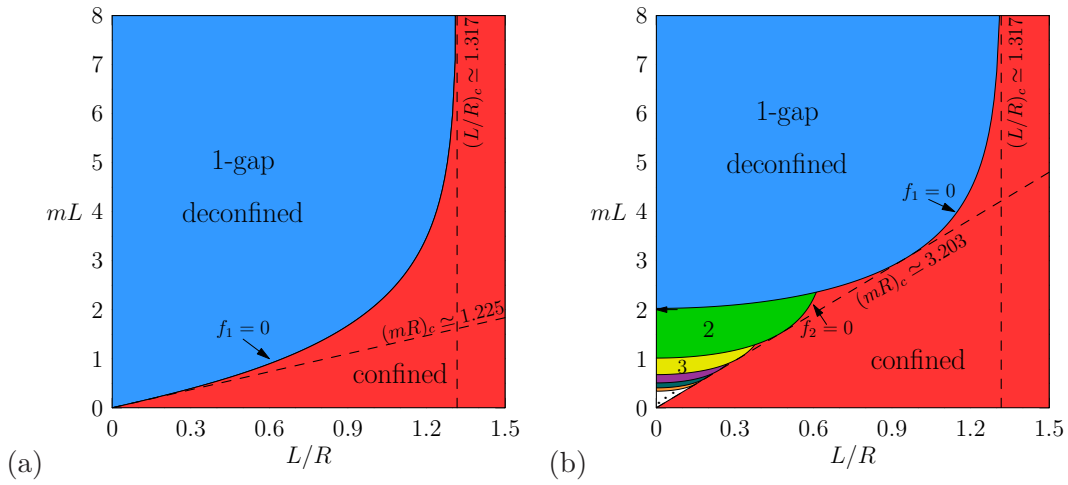

Figure 4. The phase diagrams in $(L/R, mL)$ coordinates for (a) $N_f = 1$ and (b) $N_f = 2$. We have shown the transitions between the $\mathbb{Z}_p$ and $\mathbb{Z}_{p+1}$ phases along the continuation of the $f_p = 0$ line for simplicity since this seems to be a good approximation and matches the value calculated in the $\mathbb{R}^3 \times S^1$ from [8] indicated by the arrow pointing to the mL-axis.

$f(L/R, mR) \propto g(mL)$. Hence, these lines of first order transitions must asymptote to lines of constant mL.

In the $\mathbb{Z}_p$ phase, as $L/R \to 0$ we expect the gaps will grow and in this limit the density $\rho(\theta)$ in the $\mathbb{Z}_p$ phase will only have support at p equally spaced points around the circle

$$\rho(\theta) \longrightarrow \frac{1}{p}\sum_{j=0}^{p-1} \delta(\theta - 2\pi j/p) \ . \tag{3.16}$$

In this case, the line of transitions will occur for mL being the solution of the equation

$$\sum_{j=1}^{\infty} \frac{f(jpL/R, mR)}{jp} = \sum_{j=1}^{\infty} \frac{f(j(p+1)L/R, mR)}{j(p+1)} \ , \tag{3.17}$$

or more concretely since $L/R \to 0$ we can use (3.8) to get the conditions

$$\begin{aligned} &\sum_{j=1}^{\infty} \frac{1}{(jp)^2}\left(N_f K_2(pjmL) - \frac{2}{(pjmL)^2}\right) \\ &\qquad = \sum_{j=1}^{\infty} \frac{1}{(j(p+1))^2}\left(N_f K_2((p+1)jmL) - \frac{2}{((p+1)jmL)^2}\right) \ . \end{aligned} \tag{3.18}$$

The phase diagram in the $(L/R, mL)$ plane is shown in figure 4 for the two distinct cases $N_f = 1$ and $N_f = 2$. In the former case, only the phase with one gap appears which at strong coupling is identified with the de-confined phase since the centre symmetry is completely broken. For $N_f > 1$ all the $\mathbb{Z}_p$ phases appear for $p = 1, 2, \ldots$.

The transition between the confined phase and k-gap phases occurs along the $f_k = 0$ curve. The line of transitions between k-gap and $k+1$-gap phases only slightly differs from

JHEP11(2009)008

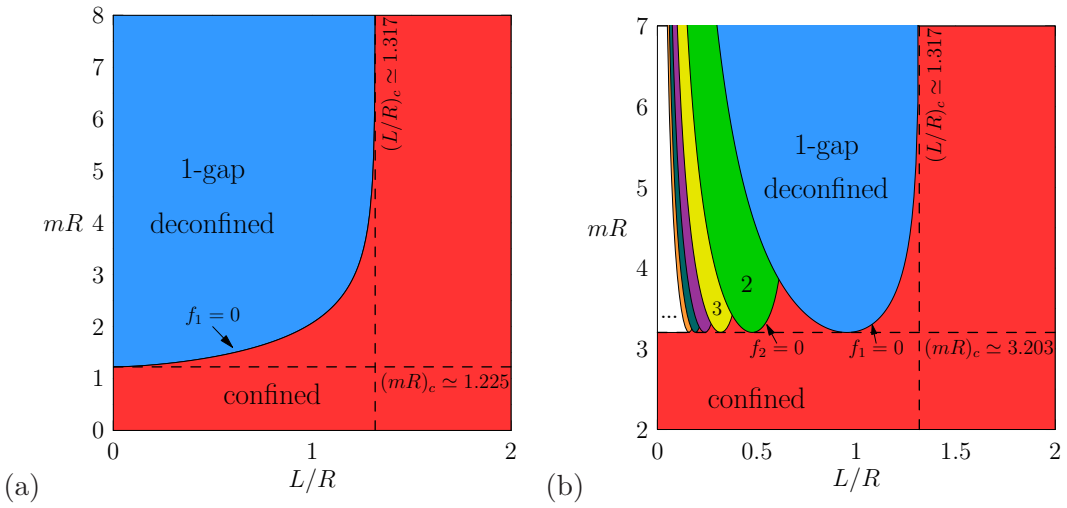

Figure 5. The phase diagram in $(L/R, mR)$ coordinates for (a) $N_f = 1$ and (b) $N_f = 2$. As above, we have shown the transitions between the $\mathbb{Z}_p$ and $\mathbb{Z}_{p+1}$ phases along the continuation of the $f_p = 0$ which seems to be a good approximation.

the $f_k = 0$ curves of figure 4. From the $\mathbb{R}^3 \times S^1$ result in [8] the transition between the 1 and 2-gap phases occurs for $mL \simeq 2.020$, where as the mL asymptote of the $f_1 = 0$ curve lies at $mL \simeq 2.027$. This difference is only barely visible in figure 4. The confined phase is always favoured below a critical line with slope $(mR)_c$ which increases with N_f. The $(L/R)_c \simeq 1.317$ line in both figures indicates the value of the deconfinement temperature of the pure SU(∞) Yang-Mills theory determined in [1].

In figure 5, we re-plot the same phase diagrams in the $(L/R, mR)$ plane. Again it is clear that only the confining phase exists for small enough mR. The basic form of the phase diagram can be understood intuitively as follows. The important point is that periodic fermions contribute positively to $f(L/R, mR)$ and consequently tend to act so as to disorder the Polyakov loop, counteracting the effect of the gauge field, and favour the confined phase. However, their effect goes away as m increases due to decoupling. Consequently, for large fermion mass m, the matter fields decouple and we recover the confinement/de-confinement of the pure gauge theory. Whereas for small mass the fermions win in the competition with the gauge fields and disorder the Polyakov loop. The most striking result of our analysis is that the confining phase extends all the way down to small L/R as long as the fermion mass in units of $1/R$ is below a critical value, $m \lesssim 1.225/R$ for $N_f = 1$, $m \lesssim 3.203/R$ for $N_f = 2$.

4 Finite N

It is useful to also consider QCD(Adj) at finite N for several reasons: (i) we can determine how the large N limit is approached and develop some intuition of when finite N results start to approximate those in the infinite N limit, (ii) with finite N and finite volume better qualitative comparison with lattice results is possible, and (iii) it is possible to compare with finite N results on $\mathbb{R}^3 \times S^1$ by considering the limit $R \to \infty$.

JHEP11(2009)008

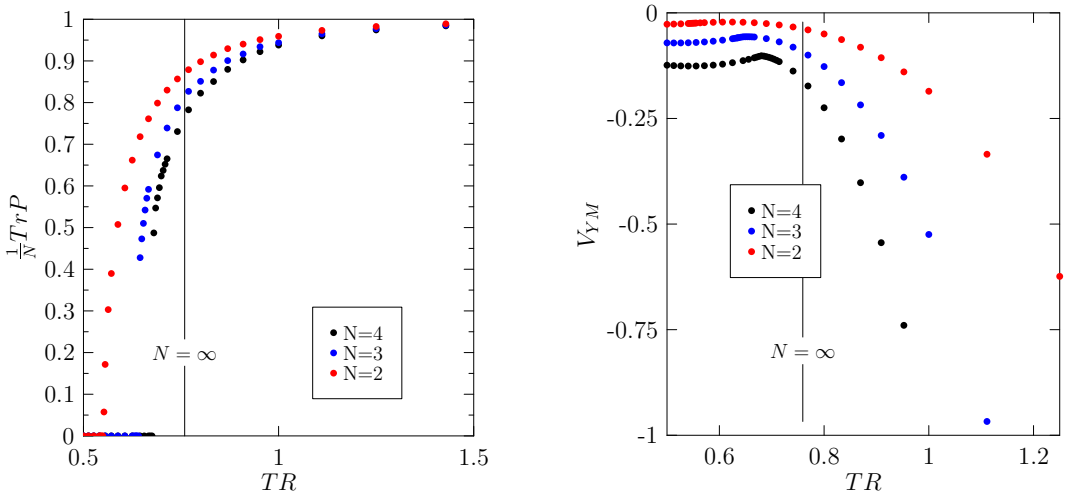

Figure 6. Yang-Mills theory for $N = 2, 3, 4$: (Left) (TR, TrP). For $N = 2$: $0.549 < T_dR < 0.552$, $N = 3$: $0.641 < T_dR < 0.645$, $N = 4$: $0.676 < T_dR < 0.680$; (Right) (TR, $V_{\rm YM}$): $V_{\rm YM}$ is the free energy density minus the const/TR Casimir term. For larger values of N this result appears increasingly compatible with a first order transition.

To build intuition on how the infinite N limit is approached it is helpful to remove fermions for the moment and consider pure Yang-Mills theory at finite N. In the strong coupling limit the de-confinement phase transition has been observed in lattice simulations and it is believed that the transition is second order for $N = 2$ and first order for $N \geq 3$ [29].

The weak-coupling analogue of the de-confinement transition of pure Yang-Mills theory is observable from perturbation theory on small volume manifolds at weak coupling. In [1] the authors calculated the de-confinement temperature from one-loop perturbation theory on $S^3 \times S^1$ and found it to occur at $T_dR = 0.75932$ in the large N limit. In [2] the same authors computed higher loop corrections to show that the large N de-confinement transition is first order in the weak coupling limit.

By numerically minimizing the Yang-Mills effective potential with respect to the Polyakov loop eigenvalues it is possible to compute the trace of the Polyakov loop order parameter as a function of the temperature as shown in figure 6 (Left) for $N = 2, 3, 4$ (See appendix C for a short discussion of numerical minimization of the effective potential for finite N). The discontinuity in the trace of the Polyakov loop is a clear indication of the de-confinement transition even for $N = 2$. Increasing N causes T_dR to approach the large N result from [1]. Near to the transition the points are separated by $\Delta L/R = 0.01$. With this resolution the $N = 2$ transition appears much smoother than for $N = 3, 4$, as we might expect from lattice results. However, it is not possible to decipher the order of the transitions for certain without taking the infinite volume limit.

The corresponding Yang-Mills effective potential (eq. (3.2) with $N_f = 0$ or $m = \infty$, which doesn't include the const/TR Casimir term) is shown in figure 6 (Right). The slight hump (most visible in the $N = 4$ result) indicates the approximate location of the de-confinement transition. It appears to become more well-defined with increasing N. Even though the finite N transitions shown in figure 6 are not genuine phase transitions since

JHEP11(2009)008

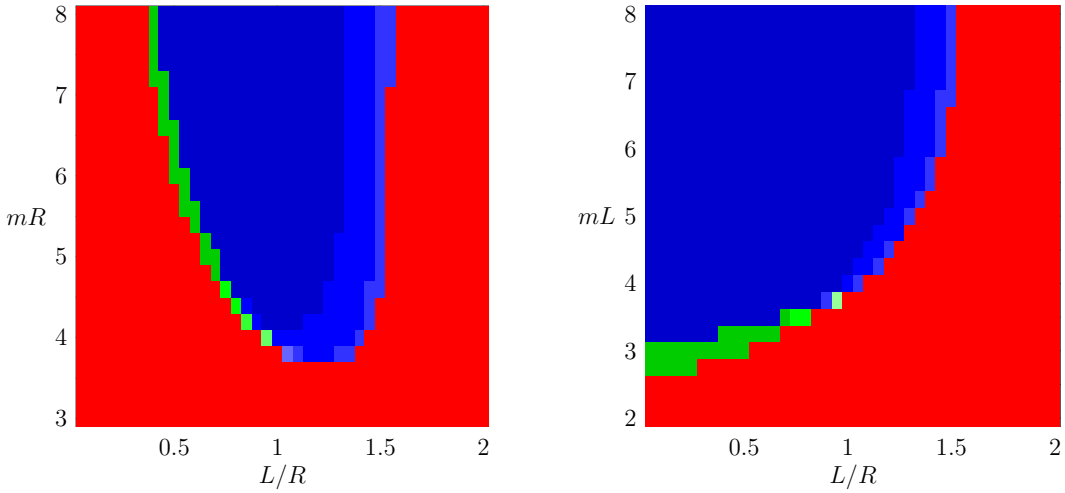

Figure 7. Phase diagram of QCD(Adj) for $N = 3$, $N_f = 4$: (Left) in the $(L/R, mR)$ plane with $3.6 < (mR)_c < 3.8$; (Right) in the $(L/R, mL)$ plane with $2.5 < (mL)_c < 2.75$.

this system does not have an infinite number of degrees-of-freedom, true transitions can be obtained by taking N or R to infinity. The sharpness of the hump in the effective potential serves as an indicator of how well the finite N transition approximates a true infinite N, or infinite volume transition.

It is important to emphasize that the use of the saddle point approximation to determine the preferred configuration of the gauge field is not strictly valid in the limit of finite N. However, one can show that it is still a reasonable approximation for purpose of obtaining the phase diagram, even for $N = 2, 3$, by plotting the effective action in the complete configuration space of the θ_i. The effective action has clear minima in the configuration space corresponding to the eigenvalues obtained with the saddle point approximation. The competition with other configurations is minimal. For L/R below $(L/R)_c$ there is a clear distinction between the confined and gapped phases which can be shown by performing the integrals over the gauge fields to obtain the partition function, Z, then plotting $e^{-S}\mathrm{Tr}P/Z$ in the full configuration space and considering a small radius around the values of the θ_i corresponding to the minima of the effective action. Above $(L/R)_c$ the fluctuations of the Polyakov loop in the full configuration space of the θ_i are more severe, but taking the average in a small radius around the configurations determined by the saddle point approximation still results in $\langle \mathrm{Tr}P \rangle = 0$. The fact that the integrals over the gauge field can be solved numerically serves as a check of the results of the saddle point approximation. However, expectation values of the Polyakov loop, for example, will always be zero, so it is important to find the eigenvalues from the saddle point approximation, and compare with plots of $e^{-S}\mathrm{Tr}P/\int [d\theta] e^{-S}$, as a function of the θ_i, such that the different $Z(N)$ phases can be distinguished. Using the saddle point approximation serves as a means of obtaining sharper phase transitions than would be observed by performing the full integrals over the gauge field configurations. It additionally picks out eigenvalues for a single minimum of the effective potential, avoiding the issue of finding a suitable order parameter for distin-

JHEP11(2009)008

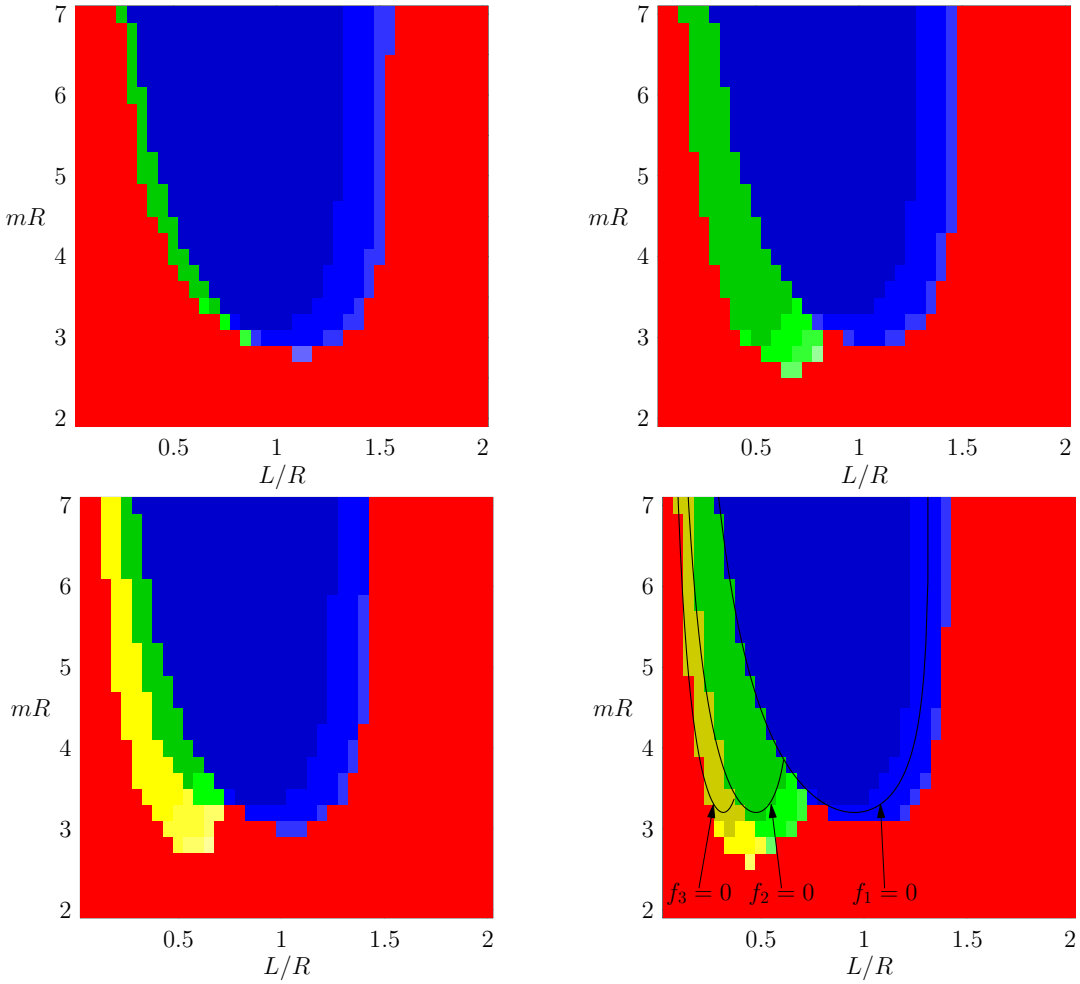

Figure 8. Phase diagram of QCD(Adj) for $N_f = 2$ in the $(L/R,\, mR)$ plane: (Top Left) $N = 3$: $2.6 < (mR)_{c\to d} < 2.8$; (Top Right) $N = 4$: $2.8 < (mR)_{c\to d} < 3.0$; (Bottom Left) $N = 5$: $2.8 < (mR)_{c\to d} < 3.0$; (Bottom Right) $N = 6$: $3.0 < (mR)_{c\to d} < 3.2$. The $f_n = 0$ curves indicate the lines of transition for the $N = \infty$ result.

guishing the $Z(N)$ vacua (or the relevant subgroup) which would otherwise be necessary since averaging over the full configuration space gives $\langle \mathrm{Tr}P \rangle = 0$ in all phases.

For QCD(Adj) at finite N we can perform an analysis similar to what was done in the case of large N. The effective potential has the exact same form except that we can't solve the path integral using the saddle point approximation unless N is large enough. Since we don't know when this is true we again use numierical minimization.

Consider SU(3) QCD(Adj). The phase diagram for $N_f = 4$ Majorana flavours in the $(L/R, mR)$ plane is shown in figure 7 (Left), and in the $(L/R, mL)$ plane in figure 7 (Right). The phases are defined according to the value of $\mathrm{Tr}P$. The confined (red) phase has $\mathrm{Tr}P^k = 0$ for all k. The 2-gap (green) phase can be distinguished from the de-confined or 1-gap (blue) phase in either of two ways: 1) The 2-gap phase has $\left|\mathrm{Tr}P^2\right| > |\mathrm{Tr}P|$, whereas the de-confined phase has $|\mathrm{Tr}P| > \left|\mathrm{Tr}P^2\right|$, 2) The 2-gap phase has $\mathrm{Proj}_{\mathbb{Z}_3}\mathrm{Tr}P < 0$ whereas the

JHEP11(2009)008

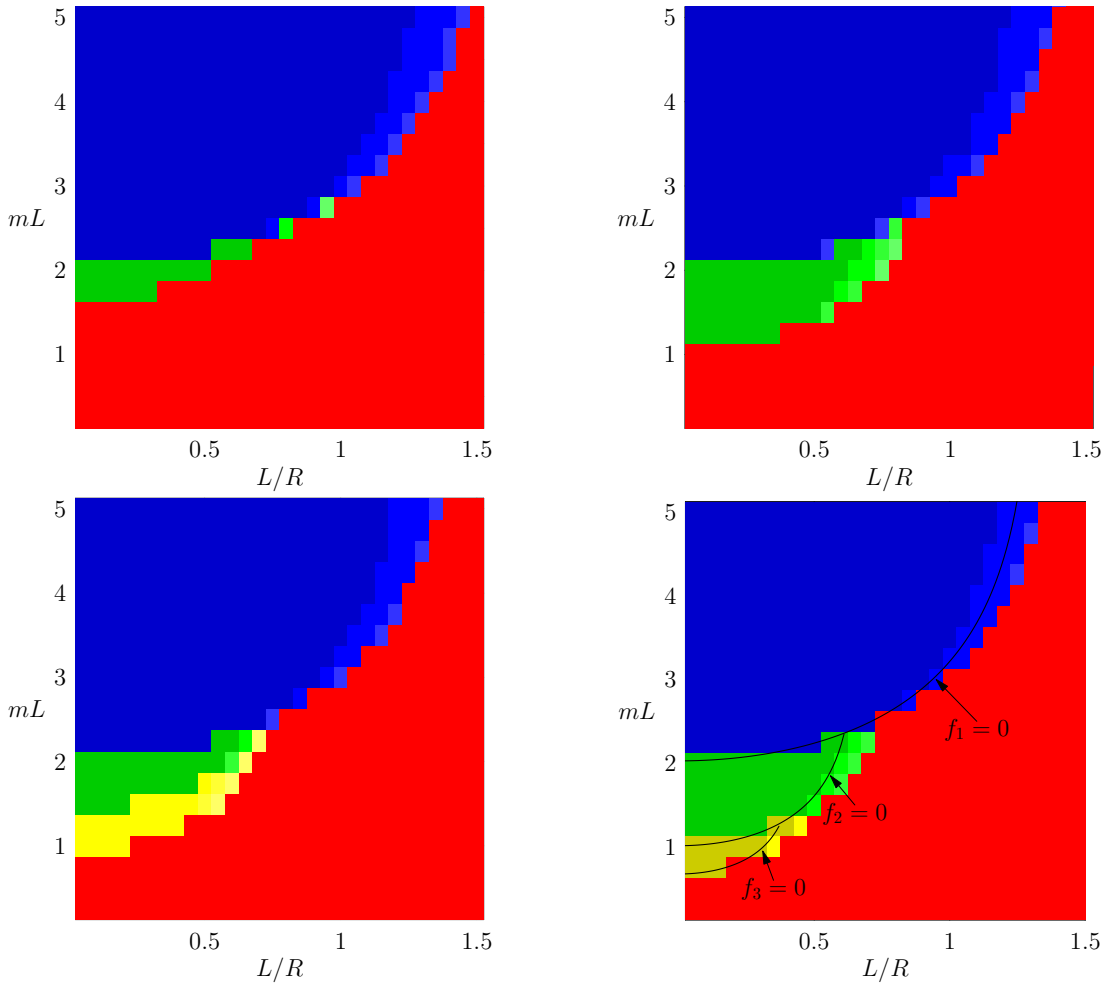

Figure 9. Phase diagram of QCD(Adj) for $N_f = 2$ in the $(L/R,\, mL)$ plane: (Top Left) $N = 3$: $1.5 < (mL)_c < 1.75$; (Top Right) $N = 4$: $1.0 < (mL)_c < 1.25$; (Bottom Left) $N = 5$: $0.75 < (mL)_c < 1.0$; (Bottom Right) $N = 6$: $0.5 < (mL)_c < 0.75$. The $f_n = 0$ curves indicate the lines of transition for the $N = \infty$ result.

de-confined phase has $\mathrm{Proj}_{\mathbb{Z}_3}\mathrm{Tr}P > 0$, where $\mathrm{Proj}_{\mathbb{Z}_3}$ indicates projection onto the nearest $\mathbb{Z}_3$ axis. Darker shading in a k-gap phase indicates a greater magnitude of $\left|\frac{1}{N}\mathrm{Tr}P^k\right|$. The pure Yang-Mills theory transition is visible at large mR for $1.55 < (L/R)_{c\to d} < 1.6$ in approximate agreement with the $N = 3$ result in figure 6. For small enough mR phase transitions are avoidable for all L/R. The critical value $(mR)_{\mathrm{crit}}$ below which $\mathbb{Z}_N$ symmetry-breaking phase transitions are absent is less for smaller N_f, but the overall shape of the phase diagram is otherwise qualitatively similar.

To see how the large N phase diagram unfolds it is useful to also consider the phase diagrams for $N = 4, 5, 6$. To compare with the $\mathbb{R}^3 \times S^1$ results in [8] we consider $N_f = 2$. The phase diagrams of $N = 3, 4, 5, 6$ QCD(Adj) are shown in the $(L/R, mR)$ plane in figure 8. As N is increased a new phase is formed for each odd N. For $N = 3$ this phase is the 2-gap phase with $\left|\mathrm{Tr}P^2\right| > |\mathrm{Tr}P|$. For $N = 5$ the new phase is the 3-gap (yellow) phase

JHEP11(2009)008

with $\left|\mathrm{Tr}P^3\right| > \left|\mathrm{Tr}P^2\right|, |\mathrm{Tr}P|$. For even N the phases fan out into the region of small L/R. But, for $N \geq 7$ the phase diagram gets even more complicated. For example, from [8] we know that for $N = 7$ it is possible to have two different 3-gap phases, one which maximizes $\left|\mathrm{Tr}P^3\right|$ and the other which maximizes $\left|\mathrm{Tr}P^4\right|$. However, if $N \mod k = 0$ then there is always a k-gap phase for which the eigenvalues are distributed in k evenly spaced clumps containing N/k eigenvalues per clump such that $\mathrm{Tr}P^k \neq 0$ and $\mathrm{Tr}P^l = 0$ for $l \neq k$. If $N \mod k \neq 0$ then there is still a k-gap phase with k clumps of eigenvalues and for which $\left|\mathrm{Tr}P^k\right| > \left|\mathrm{Tr}P^l\right|$ for l not a multiple of k. We suspect the other types of k-gap phases to result as a consequence of the decreased symmetry of the finite N theory, and conjecture that they should not be present in limit $N \to \infty$.

As N is increased the new phases extend down into lower values of (mR) than the de-confined phase, however when the next phase is formed the previous phases are dragged up into regions of larger (mR). This is what we expect given that the critical mass in the $N \to \infty$ limit occurs at $mR = 3.203$ for all the gapped phases. This phenomenon is particularly clear by examination of $(mR)_{c\to d}$ of the de-confined phase for $N = 3, 4, 5, 6$ in figure 8, which shows a steady increase in $(mR)_{c\to d}$ from $2.6 < (mR)_{c\to d} < 2.8$ for $N = 3$ to $3.0 < (mR)_{c\to d} < 3.2$ for $N = 6$.

It serves as a useful check to compare quantitatively with the results on $\mathbb{R}^3 \times S^1$ in [8]. This can be done by plotting the phase diagram in the $(L/R, mL)$ plane and considering the limit $L/R \to 0$. The phase diagrams for $N = 3, 4, 5, 6$ in the $(L/R, mL)$ plane are shown in figure 9. Taking the limit $L/R \to 0$ in these phase diagrams shows precise agreement with the $\mathbb{R}^3 \times S^1$ results in [8] for the values of mL at which the transitions occur. Away from the limit of small L/R the phases do not take the precise Polyakov loop eigenvalues which are determined for $\mathbb{R}^3 \times S^1$ in [8], rather the eigenvalues spread out slowly around the circle as L/R is increased, causing the magnitude $|\mathrm{Tr}P|$ to decrease.

4.1 Comparison with lattice results of Cossu and D'Elia

To connect with strong coupling results it is useful to qualitatively compare the phase diagram on $S^3 \times S^1$ to that from the recent lattice simulations in [10]. In [10] the authors also consider QCD(Adj) with periodic boundary conditions on fermions for the purpose of checking the volume dependence of the phase diagram. They obtain results for $N = 3$ and $N_f = 4$ (or $N_f^D = 2$ Dirac flavours). To compare with their results we calculated the phase diagram on $S^3 \times S^1$ in the $(mR, R/L)$ plane as shown in figure 10 (Left). The boundaries of the 2-gap phase correspond to the expected lines of transition in the limit of large R, i.e. the $\mathbb{R}^3 \times S^1$ result. With permission of the kind authors of [10] we show their phase diagram in the (ma, β) plane in figure 10 (Right), where m is the fermion mass, a is the lattice spacing, and β is the lattice parameter which goes like the inverse coupling $\beta = 2N/g^2$. It is important to note that this quantity is frequently confused with L (which is often also called β), however the lattice $\beta = 2N/g^2$ goes more like $1/L$. Obtaining a more quantitative relationship between β and L would allow for an even better comparison than what we have shown.

In the lattice phase diagram of figure 10 (Right) it is unclear whether or not the de-confined phase persists into the chiral limit. In the perturbative phase diagram of figure 10

JHEP11(2009)008

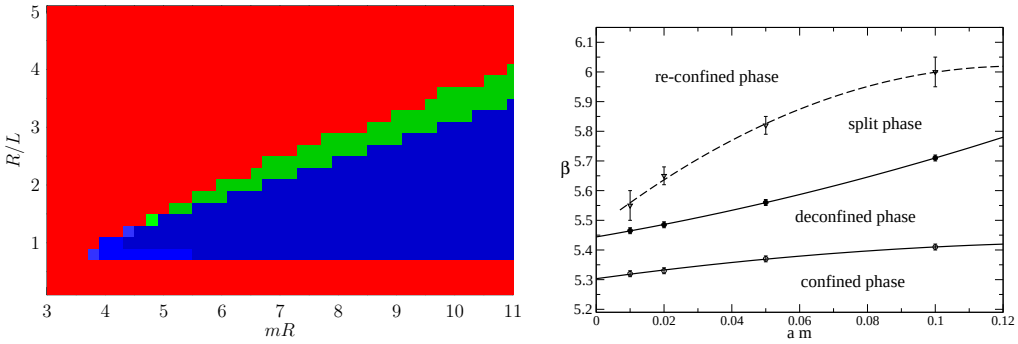

Figure 10. QCD(Adj) for $N = 3$, $N_f = 4$: (Left) $(mR,\, L/R)$. $L = 2\pi R_{S^1}$. Only the confined phase persists for $mR \lesssim 3.6$; (Right) Results from lattice simulations of Cossu and D'Elia [10] on a $16^3 \times L_c$ lattice. Here β is related to the inverse coupling $\beta = 2N/g^2$.

(Left) it does not, however, it is possible that in the case of more strongly interacting adjoint fermions the de-confined phase drops down to lower values of mR. One thing which may help answer this question is to plot the lattice phase diagram in the $(mL_s, L_s/L_t)$ plane, as it may show a clearer trend.

It is interesting to compare as well with the lattice phase diagram which results from adding a single double trace term to the pure gauge theory action [6, 7]. The phase diagrams for these theories seem to suggest that the confined phase passes through (i.e., the strong and weak-coupling confined phases are connected) when the double trace term is strong enough. The double trace term, which is approximately the contribution of static massive adjoint fermions, is given by $h\mathrm{Tr}_{\mathrm{adj}}P$ for $N = 3$, where larger magnitudes of h correspond to smaller fermion mass.[7]

Another remarkable similarity between the $S^3 \times S^1$ result and the lattice results [10] of Cossu and D'Elia is that there is good qualitative agreement for $\mathrm{Tr}P$ as a function of L for a fixed value of the fermion mass. In figure 11 we show $\mathrm{Tr}P$ as a function of the length of the temporal direction. The $S^3 \times S^1$ result in the $(L/R, \frac{1}{3}\mathrm{Proj}_{\mathbb{Z}_3}\mathrm{Tr}P)$ plane is in figure 11 (Left). The lattice result of [10] in the $(\mathrm{Re}\left[\mathrm{Tr}P\right], \mathrm{Im}\left[\mathrm{Tr}P\right])$ plane for $16^3 \times L_c$ lattices with increasing length L_c of the temporal dimension is given in figure 11 (Right). What is remarkable about this comparison is that the perturbative result appears to capture even some fine details of the phase diagram obtained on the lattice including microscopic changes in the magnitude of $\mathrm{Tr}P$. The sharp discontinuity in $\mathrm{Tr}P$ at the transition to and from the 2-gap phase, and the slow drop in $\mathrm{Tr}P$ in the de-confined phase as the confined phase is approached, seem to agree rather well.

It might, at first, seem surprising that agreement between the lattice calculation on $(S^1)^4$ and our calculation on $S^3 \times S^1$ is so good since these spaces have different first homotopy groups. However, 3 of the circles of the torus in the lattice calculation are large and so one might expect that the one remaining small circle plays the dominant role in determining the phase structure.[8] In addition, it seems that the phase diagram doesn't

[7] More information on double trace deformations can be found in [30–32].

[8] We wish to thank Mithat Unsal for useful discussions on this topic.

JHEP11(2009)008

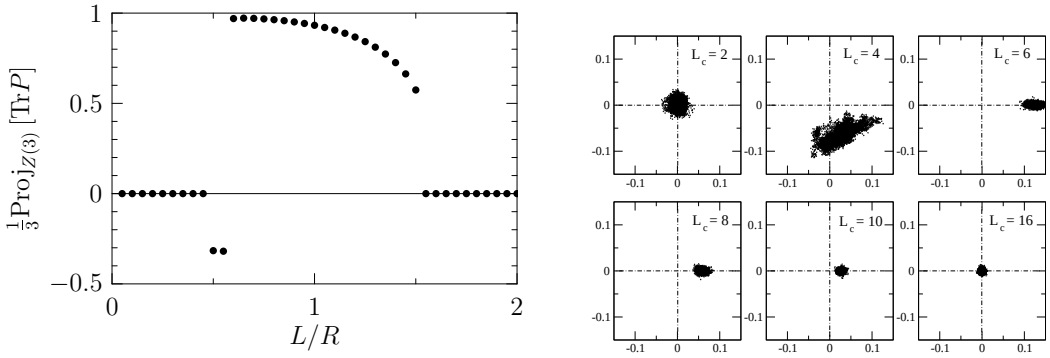

Figure 11. QCD(Adj) for $N = 3$, $N_f = 4$: (Left) Results from perturbation theory in $(L/R,$ $\frac{1}{3}\mathrm{Proj}_{\mathbb{Z}_3}\mathrm{Tr}P)$ plane. $(mR) = 6$; (Right) Results from lattice simulations of Cossu and D'Elia [10] in the $(\mathrm{Re}\,[\mathrm{Tr}P]\,, \mathrm{Im}\,[\mathrm{Tr}P])$ plane on $16^3 \times L_c$ lattices for $\beta = 5.75$ and $am = 0.10$.

change much as the coupling strength is increased from the weakly interacting limit to the strongly interacting limit when considering the phase diagram in terms of patterns of $\mathbb{Z}_N$ breaking. This is not necessarily the case for all observables.

5 Discussion

It is important to clarify the implications of our results for the issue of volume independence. The latter relies on the fact that the theory is in the confining phase with unbroken centre symmetry. Our result show that at weak coupling on $S^3 \times S^1$ the confining phase persists in the limit $L/R \to 0$ as long as the fermion mass is below a critical value in units of $1/R$, i.e. $1.225/R$ for $N_f = 1$, $3.203/R$ for $N_f = 2$. The critical mass increases with increasing N_f. Of course, our result is valid on a small S^3 and the interesting question is what happens to the critical mass as one moves to strong coupling by taking $R > 1/\Lambda_{\mathrm{QCD}}$.

The general analysis presented in this paper could just as well be applied to many other theories. For example, it is straightforward to consider QCD(Adj) with anti-periodic boundary conditions which is of interest since lattice simulations have been done [33, 34], as well as analytical calculations [35], which suggest the presence of a conformal window. It would also be interesting to consider symmetric and antisymmetric representation fermions and compare with related lattice results [36]. Interesting also, would be applications to softly broken $\mathcal{N} = 4$ theory, since there are several fermions and scalars and more complicated mass hierarchies are possible leading to more complicated phase diagrams. Whether a connection could be made with the string theory dual remains to be seen. In particular, it would be interesting to understand how the confinement/de-confinement transitions can occur with periodic boundary conditions for the fermions suggesting that it is not a Hawking-Page transition in AdS. The other related issue is how the nature of the transition changes as interactions are turned on and one moves to strong coupling. As we mentioned in the introduction, for pure gauge theory the 3-loop calculation in [2] shows that the transition is first order and occurs at a lower termperature, *i.e.* larger L/R,

JHEP11(2009)008

than the non-interacting Hagedorn transition. Unfortunately it will be very difficult to generalize the calculation of [2] to include massive fermions.

Calculations on $S^3 \times S^1$ can be used to define better the extent of perturbative validity of orientifold planar equivalence [37, 38], which is a large N equivalence of QCD(Adj) and QCD with symmetric/antisymmetric representation fermions. The same can be done for orbifold planar equivalence [39, 40], the equivalence of QCD(Adj) and QCD with bifundamental representation fermions. In both cases a comparison of large N phase diagrams is possible, and perhaps some observables could be compared. The one-loop effective potential and phase diagrams for QCD(Adj/AS/S) on $S^3 \times S^1$ with massless fermions were computed in the very clearly written papers [26, 41]. One could also study QCD (fundamental representation fermions) and incorporate a finite chemical potential. However, in this case one has to confront the sign problem. It would be interesting to compare a phase-quenched result (demanding a real fermion determinant) on $S^3 \times S^1$ with results from the several different techniques for dealing with the sign problem in QCD at various coupling strengths, a diverse sampling of which can be found in [42–48].

There are several things that might be done to allow for better comparison of weak-coupling results on $S^3 \times S^1$ to lattice results. Using the two-loop renormalization group equation to give a fitting function for the relationship between the lattice parameter $\beta = 2N/g^2$ and the length L of S^1 would allow for more quantitative comparisons. More lattice results on different volumes and for various N would show if phase diagrams are consistently similar. In particular, we see a pattern emerging that suggests that for QCD(Adj) with finite even N there are $N/2$ gapped phases (including the de-confined phase) with the property that $\left|\mathrm{Tr}P^k\right| > \left|\mathrm{Tr}P^l\right|$ in a k-gap phase for l not a multiple of k, and for N odd there are $(N+1)/2$ gapped phases with this property (narrow regions of additional phases are also possible). On the analytical side interactions might be included in the weak-coupling effective potential by working out higher loop orders. In addition, to compare even better with lattice results the theory can be put on the torus. The one-loop effective potential for QCD(Adj) with massive fermions was computed on $\mathbb{R}^d \times T^n$ in [49] (see also [50]).

Acknowledgments

Our understanding of the presented results relies heavily on relevant discussions with several colleagues. We would like to thank Barak Bringoltz, Massimo D'Elia, Ari Hietanen, Biagio Lucini, Agostino Patella, and Antonio Rago for helpful discussions on comparing with lattice results. In particular we would like to thank Guido Cossu and Massimo D'Elia for allowing us to use their figures in this paper, and to thank Massimo D'Elia for discussions of their lattice results. We would also like to thank Barak Bringoltz and Ari Hietanen for discussing their related lattice results. We are grateful to Biagio Lucini and Antonio Rago for discussions on the analysis of phase transitions. We are also grateful to Adi Armoni, Michael Ogilvie, and Mithat Ünsal for discussions on the implications to volume independence, and to Carlos Hoyos, for discussing his related calculation on the torus. Many of these discussions took place during the fruitful Large N conference in Swansea,

JHEP11(2009)008

during which progress was made towards the completion of this work. TJH would like to acknowledge the support of STFC grant. ST/G000506/1.

A Spherical harmonics

In this appendix we collect together results for the spectra of various Laplace operators on a sphere S^d.

First of all the scalar Laplace equation is solved by generalized spherical harmonics,

$$\Delta^{(s)} Y_{\ell,\vec{m}}(\hat{\Omega}) = -\varepsilon_l^{(s)2} Y_{\ell,\vec{m}}(\hat{\Omega}) \ . \tag{A.1}$$

The eigenvalues are

$$\varepsilon_l^{(s)2} = \ell(\ell+d-1)R^{-2} \ , \tag{A.2}$$

and the degeneracy is

$$d_\ell^{(s)} = \frac{(2\ell+d-1)(\ell+d-2)!}{\ell!(d-1)!}, \tag{A.3}$$

where the angular momentum $\ell = 0, 1, \ldots$.

Following [51] the eigenvalues of the vector Laplacian $\Delta^{(v)}$ on vector fields are obtained by separation of the longitudinal (L) and transverse (T) components. The spatial gauge field is thus decomposed $A_i = B_i + C_i$, where B_i is the transverse component with $\nabla_i B_i = 0$, and C_i is the longitudinal component with $C^i = \nabla^i \chi$.

The vector Laplacian acting on the longitudinal component C_i has the same spectrum as for the scalar Laplacian because

$$\left(\nabla^i \nabla_i \delta^j_k - R^j{}_k\right) \nabla_j \chi = \nabla_k \left(\nabla^i \nabla_i \chi\right) \ , \tag{A.4}$$

except that the $\ell = 0$ mode is missing:

$$\varepsilon_\ell^{(v,L)2} = \ell(\ell+d-1)R^{-2}, \tag{A.5}$$

for $\ell = 1, 2, \ldots$, and

$$d_\ell^{(v,L)} = \frac{(2\ell+d-1)(\ell+d-2)!}{\ell!(d-1)!}. \tag{A.6}$$

The eigenvalues and degeneracy of the vector Laplacian on the transverse components B_i are

$$\varepsilon_\ell^{(v,T)2} = \big(\ell(\ell+d-1)+d-2\big)R^{-2}\,, \tag{A.7}$$

and

$$d_\ell^{(v,T)} = \frac{\ell(\ell+d-1)(2\ell+d-1)(\ell+d-3)!}{(d-2)!(\ell+1)!} \ . \tag{A.8}$$

for $\ell = 1, 2, \ldots$.

The Laplacian on spinors is given by

$$\Delta^{(f)} = \gamma^i \gamma^j \nabla_i \nabla_j = g^{ij} \nabla_i \nabla_j - \frac{1}{4} R\,, \tag{A.9}$$

where $\mathcal{R}$ is the scalar curvature of the sphere and

$$\nabla_i = \partial_i + \Gamma_i \tag{A.10}$$

is the covariant derivative on spinors with spin connection Γ_i. The eigenvalues and degeneracy [52–54] are

$$\varepsilon_l^{(f)2} = \big(\ell + \frac{d}{2}\big)^2 R^{-2}\,, \tag{A.11}$$

and

$$d_\ell^{(f)} = \frac{2\big(d+\ell-2\big)!}{(\ell-1)!(d-1)!}\,, \tag{A.12}$$

where $\ell = 1, 2, \ldots$.

B The Abel-Plana formula

In this appendix, we prove the version of the Abel-Plana formula quoted in the main text (2.16). The idea is to represent the sum on left-hand side as a contour integral:

$$\sum_{\ell=0}^{\infty} f(\ell+\frac{1}{2}) = \frac{i}{2}\int_{\mathcal{C}} dz\, f(z)\tan(\pi z)\,, \tag{B.1}$$

where $\mathcal{C}$ is the contour illustrated in figure 12. In our case, the function $f(z)$ has square root branch points at $z = \pm imR$. Using the above we have

$$\sum_{\ell=0}^{\infty} f(\ell+\frac{1}{2}) - \int_0^\infty dx\, f(x) = \frac{1}{2i}\int_0^{\infty+i\epsilon} dz\, f(z)\big(\tan(\pi z) - i\big) - \text{c.c.} \tag{B.2}$$

Now we can rotate the contour here that runs from the origin out to infinity over the poles so that it runs from the origin to $i\infty$ to the right of the branch point of $f(z)$ at imR. This gives the right-hand side as

$$-\,i\int_0^\infty dx\,\frac{f(ix+\epsilon)}{e^{2\pi x}+1} - \text{c.c.} \tag{B.3}$$

Hence, we have proved that

$$\sum_{\ell=0}^{\infty} f\left(\ell+\frac{1}{2}\right) = \int_0^\infty dx\, f(x) - i\int_0^\infty dx\,\frac{f(ix+\epsilon) - f(-ix-\epsilon)}{e^{2\pi x}+1}\,. \tag{B.4}$$

which is the formula (2.16) in the text.

C Numerical minimization

In the finite N calculations of the phase diagram it was necessary to numerically minimize the effective potential. This was not trivial as it is difficult to find an algorithm that will always find the global minimum of an arbitrary function. Two techniques which proved most useful were the Random Search and Differential Evolution numerical minimization routines

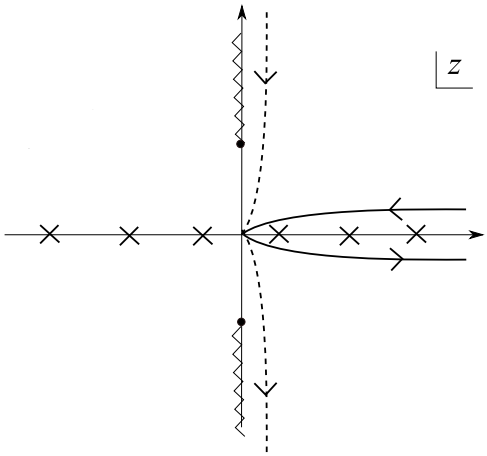

Figure 12. The contour used in the derivation of the Abel-Plana formula.

implemented in Mathematica, which are reviewed in [55]. Increasing the number of search points improves the chances of obtaining the global minimum. Somewhat surprisingly in most cases just 5 search points were enough to obtain the minimum accurate to around 13 digits for $N = 3$. It is only slightly less accurate when considering $N = 4, 5, 6$. The addition of the mass term to the effective potential actually makes the minimization easier. The pure gauge theory plots required many more search points, between 500 and 1500.

It was not possible to obtain reliable minimization of the effective potential when there were terms represented as an infinite series. Therefore it was necessary to put all infinite series in a non-series expression, either by solving them, or converting them into integral forms using the Abel-Plana formula.

As this type of calculation doesn't have much history (however, the same procedure was used in [8]) there is a lot of room for improvement in technique.

It is additionally important to perform checks of the saddle point approximation by plotting the relevant observables as a function of the configuration space of the θ_i as discussed in the finite N section.

References

[1] O. Aharony, J. Marsano, S. Minwalla, K. Papadodimas and M. Van Raamsdonk, *The Hagedorn/deconfinement phase transition in weakly coupled large-N gauge theories*, *Adv. Theor. Math. Phys.* **8** (2004) 603 [hep-th/0310285] [SPIRES].

[2] O. Aharony, J. Marsano, S. Minwalla, K. Papadodimas and M. Van Raamsdonk, *A first order deconfinement transition in large-N Yang- Mills theory on a small 3-sphere*, *Phys. Rev.* **D 71** (2005) 125018 [hep-th/0502149] [SPIRES].

[3] J. Hallin and D. Persson, *Thermal phase transition in weakly interacting, large-N_c QCD*, *Phys. Lett.* **B 429** (1998) 232 [hep-ph/9803234] [SPIRES].

[4] B. Sundborg, *The Hagedorn transition, deconfinement and $N = 4$ SYM theory*, *Nucl. Phys.* **B 573** (2000) 349 [hep-th/9908001] [SPIRES].

JHEP11(2009)008

[5] E. Witten, *Anti-de Sitter space, thermal phase transition and confinement in gauge theories*, *Adv. Theor. Math. Phys.* **2** (1998) 505 [hep-th/9803131] [SPIRES].

[6] J.C. Myers and M.C. Ogilvie, *New phases of* SU(3) *and* SU(4) *at finite temperature*, *Phys. Rev.* **D 77** (2008) 125030 [arXiv:0707.1869] [SPIRES].

[7] C. Wozar, T. Kastner, B.H. Wellegehausen, A. Wipf and T. Heinzl, *Inverse Monte-Carlo and demon methods for effective polyakov loop models of* SU(N)*-YM*, arXiv:0808.4046 [SPIRES].

[8] J.C. Myers and M.C. Ogilvie, *Phase diagrams of* SU(N) *gauge theories with fermions in various representations*, *JHEP* **07** (2009) 095 [arXiv:0903.4638] [SPIRES].

[9] P.F. Bedaque, M.I. Buchoff, A. Cherman and R.P. Springer, *Can fermions save large-N dimensional reduction?*, arXiv:0904.0277 [SPIRES].

[10] G. Cossu and M. D'Elia, *Finite size phase transitions in QCD with adjoint fermions*, *JHEP* **07** (2009) 048 [arXiv:0904.1353] [SPIRES].

[11] B. Bringoltz, *Large-N volume reduction of lattice QCD with adjoint Wilson fermions at weak-coupling*, *JHEP* **06** (2009) 091 [arXiv:0905.2406] [SPIRES].

[12] B. Bringoltz and S.R. Sharpe, *Non-perturbative volume-reduction of large-N QCD with adjoint fermions*, *Phys. Rev.* **D 80** (2009) 065031 [arXiv:0906.3538] [SPIRES].

[13] P. Kovtun, M. Ünsal and L.G. Yaffe, *Volume independence in large-N_c QCD-like gauge theories*, *JHEP* **06** (2007) 019 [hep-th/0702021] [SPIRES].

[14] G. Boyd et al., *Thermodynamics of* SU(3) *lattice gauge theory*, *Nucl. Phys.* **B 469** (1996) 419 [hep-lat/9602007] [SPIRES].

[15] T. Eguchi and H. Kawai, *Reduction of dynamical degrees of freedom in the large N gauge theory*, *Phys. Rev. Lett.* **48** (1982) 1063 [SPIRES].

[16] L.G. Yaffe, *Large-N limits as classical mechanics*, *Rev. Mod. Phys.* **54** (1982) 407 [SPIRES].

[17] G. Bhanot, U.M. Heller and H. Neuberger, *The quenched Eguchi-Kawai model*, *Phys. Lett.* **B 113** (1982) 47 [SPIRES].

[18] V.A. Kazakov and A.A. Migdal, *Weak coupling phase of the Eguchi-Kawai model*, *Phys. Lett.* **B 116** (1982) 423 [SPIRES].

[19] M. Okawa, *Monte Carlo study of the Eguchi-Kawai model*, *Phys. Rev. Lett.* **49** (1982) 353 [SPIRES].

[20] B. Bringoltz and S.R. Sharpe, *Breakdown of large-N quenched reduction in* SU(N) *lattice gauge theories*, *Phys. Rev.* **D 78** (2008) 034507 [arXiv:0805.2146] [SPIRES].

[21] A. Gonzalez-Arroyo and M. Okawa, *A twisted model for large-N lattice gauge theory*, *Phys. Lett.* **B 120** (1983) 174 [SPIRES].

[22] M. Teper and H. Vairinhos, *Symmetry breaking in twisted Eguchi-Kawai models*, *Phys. Lett.* **B 652** (2007) 359 [hep-th/0612097] [SPIRES].

[23] T. Azeyanagi, M. Hanada, T. Hirata and T. Ishikawa, *Phase structure of twisted Eguchi-Kawai model*, *JHEP* **01** (2008) 025 [arXiv:0711.1925] [SPIRES].

[24] M. Hanada, L. Mannelli and Y. Matsuo, *Four-dimensional $N = 1$ super Yang-Mills from matrix model*, arXiv:0905.2995 [SPIRES].

[25] G. Ishiki, S.-W. Kim, J. Nishimura and A. Tsuchiya, *Testing a novel large-N reduction for $N = 4$ super Yang-Mills theory on $R \times S^3$*, *JHEP* **09** (2009) 029 [arXiv:0907.1488] [SPIRES].

JHEP11(2009)008

[26] T.J. Hollowood and A. Naqvi, *Phase transitions of orientifold gauge theories at large-N in finite volume*, *JHEP* **04** (2007) 087 [hep-th/0609203] [SPIRES].

[27] T. Hollowood, S.P. Kumar and A. Naqvi, *Instabilities of the small black hole: a view from N = 4 SYM*, *JHEP* **01** (2007) 001 [hep-th/0607111] [SPIRES].

[28] T.J. Hollowood, S.P. Kumar, A. Naqvi and P. Wild, *N = 4 SYM on S^3 with near critical chemical potentials*, *JHEP* **08** (2008) 046 [arXiv:0803.2822] [SPIRES].

[29] B. Lucini, M. Teper and U. Wenger, *Properties of the deconfining phase transition in* SU(N) *gauge theories*, *JHEP* **02** (2005) 033 [hep-lat/0502003] [SPIRES].

[30] M. Schaden, *Confinement at weak coupling*, *Nucl. Phys. Proc. Suppl.* **161** (2006) 210 [hep-th/0511046] [SPIRES].

[31] M.C. Ogilvie, P.N. Meisinger and J.C. Myers, *Exploring partially confined phases*, PoS(LATTICE 2007)213 [arXiv:0710.0649] [SPIRES].

[32] M. Ünsal and L.G. Yaffe, *Center-stabilized Yang-Mills theory: confinement and large-N volume independence*, *Phys. Rev.* **D 78** (2008) 065035 [arXiv:0803.0344] [SPIRES].

[33] A.J. Hietanen, J. Rantaharju, K. Rummukainen and K. Tuominen, *Spectrum of* SU(2) *lattice gauge theory with two adjoint Dirac flavours*, *JHEP* **05** (2009) 025 [arXiv:0812.1467] [SPIRES].

[34] L. Del Debbio, A. Patella and C. Pica, *Higher representations on the lattice: numerical simulations.* SU(2) *with adjoint fermions*, arXiv:0805.2058 [SPIRES].

[35] E. Poppitz and M. Ünsal, *Conformality or confinement: (IR)relevance of topological excitations*, *JHEP* **09** (2009) 050 [arXiv:0906.5156] [SPIRES].

[36] T. DeGrand, Y. Shamir and B. Svetitsky, *Phase structure of* SU(3) *gauge theory with two flavors of symmetric-representation fermions*, *Phys. Rev.* **D 79** (2009) 034501 [arXiv:0812.1427] [SPIRES].

[37] A. Armoni, M. Shifman and G. Veneziano, *Exact results in non-supersymmetric large-N orientifold field theories*, *Nucl. Phys.* **B 667** (2003) 170 [hep-th/0302163] [SPIRES].

[38] A. Armoni, M. Shifman and G. Veneziano, *Refining the proof of planar equivalence*, *Phys. Rev.* **D 71** (2005) 045015 [hep-th/0412203] [SPIRES].

[39] P. Kovtun, M. Ünsal and L.G. Yaffe, *Non-perturbative equivalences among large-N_c gauge theories with adjoint and bifundamental matter fields*, *JHEP* **12** (2003) 034 [hep-th/0311098] [SPIRES].

[40] P. Kovtun, M. Ünsal and L.G. Yaffe, *Necessary and sufficient conditions for non-perturbative equivalences of large-N_c orbifold gauge theories*, *JHEP* **07** (2005) 008 [hep-th/0411177] [SPIRES].

[41] M. Ünsal, *Phases of $N_c = \infty$ QCD-like gauge theories on $S^3 \times S^1$ and nonperturbative orbifold-orientifold equivalences*, *Phys. Rev.* **D 76** (2007) 025015 [hep-th/0703025] [SPIRES].

[42] G. Aarts and I.-O. Stamatescu, *Stochastic quantization at finite chemical potential*, *JHEP* **09** (2008) 018 [arXiv:0807.1597] [SPIRES].

[43] S. Hands, S. Kim and J.-I. Skullerud, *Deconfinement in dense 2-color QCD*, *Eur. Phys. J.* **C 48** (2006) 193 [hep-lat/0604004] [SPIRES].

[44] M. D'Elia, F. Di Renzo and M.P. Lombardo, *The strongly interacting quark gluon plasma and the critical behaviour of QCD at imaginary chemical potential*, *Phys. Rev.* **D 76** (2007) 114509 [arXiv:0705.3814] [SPIRES].

JHEP11(2009)008

[45] P. de Forcrand and O. Philipsen, *The chiral critical line of $N_f = 2 + 1$ QCD at zero and non-zero baryon density*, *JHEP* **01** (2007) 077 [hep-lat/0607017] [SPIRES].

[46] G. Akemann, J.C. Osborn, K. Splittorff and J.J.M. Verbaarschot, *Unquenched QCD Dirac operator spectra at nonzero baryon chemical potential*, *Nucl. Phys.* **B 712** (2005) 287 [hep-th/0411030] [SPIRES].

[47] M.G. Alford, A. Schmitt, K. Rajagopal and T. Schafer, *Color superconductivity in dense quark matter*, *Rev. Mod. Phys.* **80** (2008) 1455 [arXiv:0709.4635] [SPIRES].

[48] M.C. Ogilvie and P.N. Meisinger, *PT symmetry and QCD: finite temperature and density*, arXiv:0812.0176 [SPIRES].

[49] J.L.F. Barbon and C. Hoyos-Badajoz, *Dynamical Higgs potentials with a landscape*, *Phys. Rev.* **D 73** (2006) 126002 [hep-th/0602285] [SPIRES].

[50] P. van Baal, *QCD in a finite volume*, hep-ph/0008206 [SPIRES].

[51] L. De Nardo, D.V. Fursaev and G. Miele, *Heat-kernel coefficients and spectra of the vector laplacians on spherical domains with conical singularities*, *Class. Quant. Grav.* **14** (1997) 1059 [hep-th/9610011] [SPIRES].

[52] P. Candelas and S. Weinberg, *Calculation of gauge couplings and compact circumferences from selfconsistent dimensional reduction*, *Nucl. Phys.* **B 237** (1984) 397 [SPIRES].

[53] R. Camporesi, *The Spinor heat kernel in maximally symmetric spaces*, *Commun. Math. Phys.* **148** (1992) 283 [SPIRES].

[54] R. Camporesi and A. Higuchi, *On the eigen functions of the Dirac operator on spheres and real hyperbolic spaces*, *J. Geom. Phys.* **20** (1996) 1 [gr-qc/9505009] [SPIRES].

[55] B. Champion, *Numerical optimization in mathematica: an insider's view of NMinimize*, in the proceedings of the 2002 *World Multiconference on Systemics, Cybernetics, and Informatics (SCI2002)*, July 14–18, Orlando, Florida, U.S.A. (2002), online at http://library.wolfram.com/infocenter/Conferences/4311/.

JHEP11(2009)008